Eur J Cancer Clin Oncol, Vol. 21, No. 2, pp. 243-247, 1985.
Printed in Great Britain.

0277-5379/85$3.00+0.00
Pergamon Press Ltd.

Cell Cycle-dependent Adriamycin Uptake in Chinese Hamster Cells*

N. TOKITA and M. R. RAJU

Life Sciences Division, Los Alamos National Laboratory, University of California, Los Alamos, NM 87545, U.S.A.

Abstract—*Adriamycin fluorescence was measured by flow cytometry after exposing synchronized Chinese hamster (line CHO) cells to a fixed dose of adriamycin (ADR). Three synchrony methods were used: mitotic selection, isoleucine-deficient culture and pretreatment with low doses of ADR. Approximately a 1.6- to 2-fold increase in ADR fluorescence intensity was observed for cells in $G_2 + M$ compared to cells in G_1. An increase in ADR fluorescence was also noted for cell populations exhibiting a G_2 block after pretreatment with low-dose ADR. No significant difference in fluorescence intensity was observed for G_1 cell populations with two different volume distributions. Results suggest that the magnitude of ADR fluorescence is affected by the cell cycle distribution and that cellular susceptibility to drug-induced cytokinetic changes during exposure must also be taken into consideration when measuring ADR uptake.*

INTRODUCTION

SUSCEPTIBILITY of cells to adriamycin (anthracycline HCl, ADR) can be predicted by quantifying intracellular drug concentration after exposure to ADR [1, 2]. Reduced uptake, a manifestation of ADR-resistance, results from decreased ADR permeability across the plasma membrane [1-8] and/or from an active drug-exclusion mechanism [9]. Although ADR is known to intercalate between base pairs of DNA [10], it has been reported that only 26% of intracellular ADR is bound to DNA in Chinese hamster cells [8]. ADR fluorescence distributions measured by flow cytometry (FCM) are often complex because ADR distributions vary within a cell as well as within a cell population.

The present study was designed to obtain ADR fluorescence profiles as a function of cell cycle and to find correlations between ADR fluorescence distributions and DNA histograms. ADR fluorescence was also measured of cell populations with normal and perturbed cell cycle distributions since the magnitude of perturbation correlates with the level of intracellular ADR [11]. Attempts are also made to determine the role of cell volume in ADR fluorescence. A flow cytometer was used to measure ADR fluorescence as described previously [12].

Results indicate that G_1 cells display a narrow fluorescence distribution of low intensity whereas cells in $G_2 + M$ exhibit a broad fluorescence distribution with as much as a 2-fold increase in intensity compared to that of G_1 cells. Considerably higher ADR fluorescence intensity is also observed for cells in early S than for cells in late G_1. However, changes in cell volume appear insignificant in ADR fluorescence. A long-term ADR exposure induces changes in cell cycle distribution which results in increased magnitude of ADR fluorescence intensity.

MATERIALS AND METHODS

Chinese hamster cells (line CHO), in suspension culture, used in this study were maintained in F-10 medium supplemented with 15% newborn calf serum (NCS) and antibiotics at 37°C [13].

Three methods of cell synchrony were employed: mitotic selection [14], isoleucine deficiency [13] and ADR-induced perturbation. For mitotic selection exponentially growing (monolayered) CHO cells in culture bottles were mechanically shaken, and detached mitotic cells were collected in ice-cold medium. After adequate numbers of cells were collected, the cells were cultured in

Accepted 26 July 1984.
*This work was supported by a Grant CA 22585 from the National Cancer Institute, DHEW and by the U.S. Department of Energy.

medium at 37°C and, at various times after the beginning of incubation, aliquots of the cells were removed from the culture for ADR exposure. For the isoleucine deficiency-induced synchrony exponentially growing CHO cells in suspension were centrifuged and resuspended in isoleucine-deficient medium supplemented with 10% NCS (dialyzed) for 36 hr. The cells were then centrifuged, and the cell pellet resuspended in complete medium. At various times after release aliquots of cells were taken and exposed to ADR. For ADR-induced synchrony CHO cells in suspension (2×10^5 cells/ml) were cultured in F-10 medium containing 0.05 μg/ml ADR for 1 hr at 37°C. After exposure the cells were centrifuged, rinsed twice with phosphate-buffered salt solution (PBS) and resuspended in drug-free medium at 37°C. At various times after pre-treatment aliquots of the cells were removed from the culture and re-exposed to ADR. For each synchrony experiment part of the cells were also fixed in ethanol for DNA histogram analysis.

ADR exposures were carried out as follow: cells in suspension culture (2×10^5 cells/ml) taken at various times after the beginning of synchrony were resuspended in medium containing freshly prepared ADR (Adria Laboratories, Columbus, OH, U.S.A.) at 5 μg/ml for 1 hr at 37°C in the dark. After ADR exposure the cells were centrifuged (200 *g*, 5 min), rinsed twice with PBS, resuspended in PBS and immediately measured for intracellular ADR fluorescence by a flow cytometer FMF II [15]. Asynchronous CHO cells (2×10^5 cells/ml) similarly treated with ADR were used as a normalization marker. The argon-laser emission was set at 488 nm and the power output at this wavelength was in the range of 1-1.5 W. The samples were run at a rate of approximately 500-1000 cells/sec.

For approximate comparison of ADR fluorescence distributions the fluorescence intensity of each population was quantified on the basis of the average channel. The average channel value (ACV) of each distribution is calculated by the integral value of the distribution (the number of cells times the channel number for each channel) divided by the number of cells as follows:

$$(\Sigma_{i=a}^{i=b} iN_i) / (\Sigma_{i=a}^{i=b} N_i),$$

where N_i is the number of cells at the channel i.

DNA histograms were obtained by FCM after staining ethanol-fixed cells with mithramycin excited at 457 nm [16].

RESULTS

In order to obtain ADR fluorescence distributions of cells in G_1, S and $G_2 + M$, cells synchronized by mitotic selection were exposed to 5 μg/ml ADR for 1 hr and both DNA histograms and ADR fluorescence distributions were obtained (Fig. 1). The abscissa and the ordinate correspond to fluorescence intensity and number of cells respectively. It required approximately 8.5 hr for cells to reach the G_1/S boundary after mitotic selection. Cells in G_1 as shown by mithramycin staining display a narrow ADR fluorescence distribution with an average channel value (ACV) of 84 (8.5 hr after mitotic selection). Cells mainly in the early S region show a broad fluorescence distribution with an ACV of 133 (11.5 hr after mitotic selection), approximately 60% higher than that of cells in G_1. The ACV for cells mainly in mid-late S phase is 157 (14.5 hr after mitotic selection), approximately 90% higher than that of G_1 cells. For cells mainly in $G_2 + M$ regions

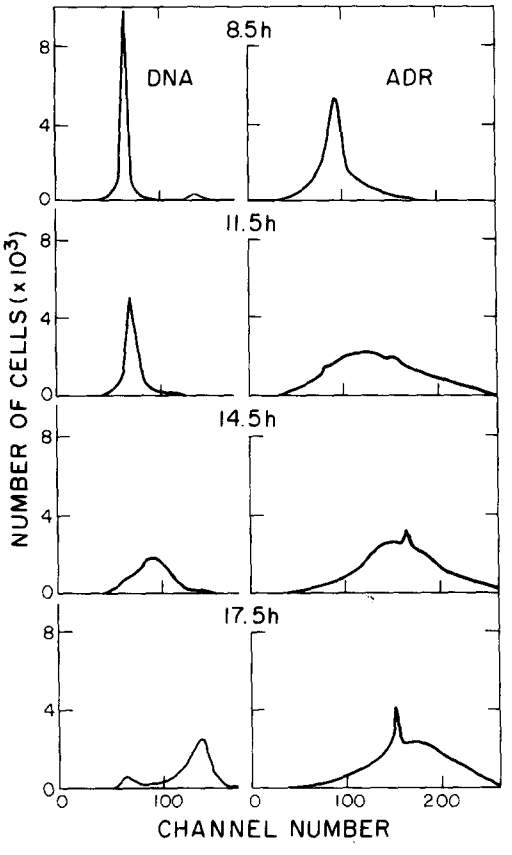

Fig. 1. DNA histograms (left) and ADR fluorescence distributions (right) for CHO cells synchronized by mitotic selection. The abscissa (channel number) corresponds to fluorescence intensity of mithramycin (DNA histograms) and ADR. Average channel values (ACV) for the ADR fluorescence distributions are 84 for cells in G_1 (8.5 hr after mitotic selection); 133 for cells in early S (11.5 hr after mitotic selection); 157 for cells in mid-late S (14.5 hr after mitotic selection); and 163 for cells in $G_2 + M$ (17.5 hr after mitotic selection).

(17.5 hr after mitotic selection) the ACV is 163, also about 90% higher than that of cells in G_1. ADR fluorescence distributions are also broad for these cells.

A similar study was carried out using CHO cells synchronized by the isoleucine-deprivation method [13] to determine the ADR fluorescence distribution of cells in specific phases of cell cycle. Figure 2 shows the DNA histograms (insert) and ADR fluorescence distributions of cells in G_1, S and G_2 + M. The ADR fluorescence for cells in G_1 also exhibits a narrow distribution as compared to those of S and G_2 + M. The ACVs for cells in G_1, S and G_2 + M were 78, 117 and 124 respectively. Thus the ACV ratios for cells in G_1, S and G_2 + M are 1, 1.5 and 1.6 respectively. The ACV ratios are somewhat different from those obtained using the mitotic selection method, probably attributable to the difference in synchrony method.

Since only a fraction of intracellular ADR is bound to the nucleus [8] and the rest remains in the cytoplasm, cells with a large volume may have a higher ADR fluorescence than those with a small volume. In order to determine the influence of cell volume in ADR uptake, G_1 cell populations of two different volume distributions were exposed to ADR and ADR fluorescence distributions measured. This was carried out by using the isoleucine deficiency-induced synchrony method [13]. After release from 36-hr culture in isoleucine-deficient medium the cell volume of G_1 cells was found to be larger than the G_1 cells of the exponentially growing population. This is partly due to increased protein synthesis [17]. The cells released from isoleucine-deficient medium continued to increase in size as the cells progressed through the G_1 phase. During the period from the early to late G_1 phase (0 and 7 hr after release) the

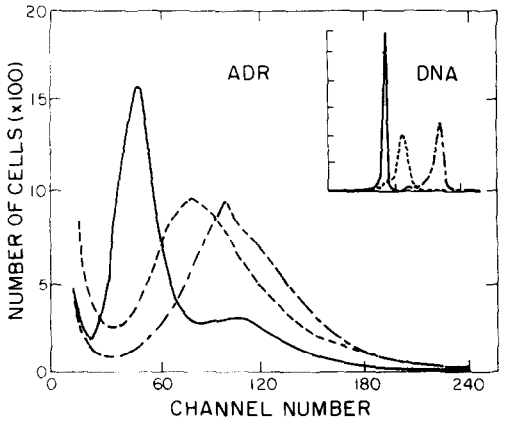

Fig. 2. ADR fluorescence distributions and DNA distributions (insert) for CHO cells synchronized by the isoleucine deficiency method. The abscissa (channel number) coresponds to fluorescence intensity of ADR and mithramycin (insert). ACVs for cells in G_1 (————), S (– – – –) and G_2 + M (— — — —) are 78, 117 and 124 respectively.

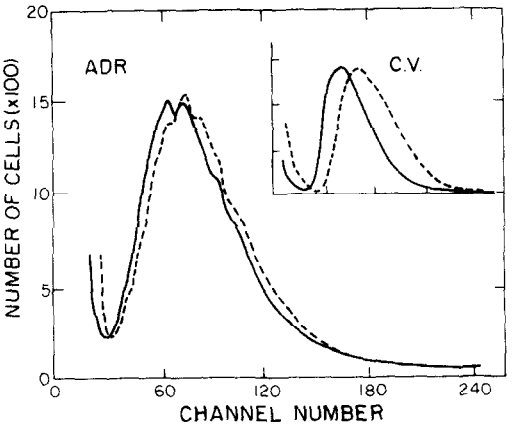

Fig. 3. ADR fluorescence distributions for CHO cells in early (————) and late (– – – –) G_1 phase. The two populations (insert) differ by 20% in cell volume but there is no significant change in ADR fluorescence.

cell volume increased by approximately 20% (Fig. 3, insert). ADR fluorescence distributions for these cells, however, are similar, suggesting that ADR fluorescence is not affected by the change in cell volume (Fig. 3).

Since it appeared from these results that cells in early S may have considerably higher ADR fluorescence than those in G_1, it seemed possible that the ADR fluorescence profile may be affected if there is a change in cell cycle distribution during the ADR exposure period. To study this effect, asynchronous cells were pretreated briefly with a low dose of ADR to induce cell cycle changes and the cells were then re-exposed to ADR at various times after pretreatment. The ADR dose used for pretreatment was so low that immediately after pretreatment no ADR fluorescence was detected by FCM. Figure 4 shows the DNA histograms and ADR fluorescence distributions for pretreated cells re-exposed to 5 μg/ml for 1 hr at various times after pretreatment. The ACV for ADR fluorescence is 102 at 0 hr (immediately after the pretreatment with 0.05 μg/ml for 1 hr). At 3 hr the ACV is 115 for cells accumulated in S and G_2 + M, an increase of 13% compared to that of 0 hr. At 6 hr, when more cells are found in late S and G_2 + M, the ACV is 118, an increase of 16%. At 9 hr, when there is a significant G_2 block, the ACV is 163, approximately 60% higher than that of 0 hr. The data indicate that a cell population with a block in G_2 will have a higher ADR fluorescence and that populations with altered cell cycle distributions will have an altered ACV.

DISCUSSION

Quantification of drug uptake as a means to predict cellular response to drugs appears attractive since the time period required for this assay would be considerably shorter than that based on colony formation. However, when

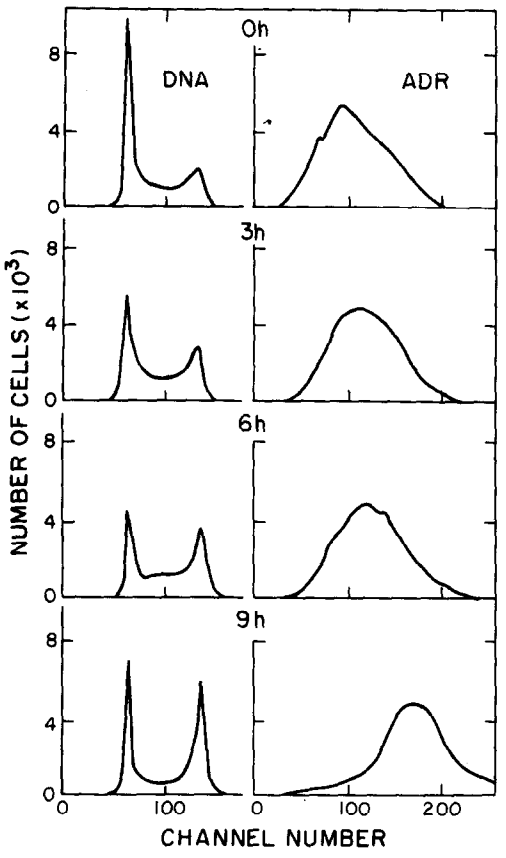

Fig. 4. DNA histograms and ADR fluorescence distributions for ADR-pretreated cells. Cells pretreated with low-dose ADR were re-exposed to a fixed dose of ADR and ADR fluorescence measured 0–9 hr after pretreatment. ACVs are 102, 115, 118 and 163 for cells re-exposed to ADR at 0, 3 6 and 9 hr after pretreatment respectively.

interpreting ADR uptake measured by ADR fluorescence intensity, various factors such as drug concentration or exposure period must be taken into consideration. ADR fluorescence distributions obtained by flow cytometry are also complex, partly due to the fact that ADR may be found in the nucleus as well as in the cytoplasm. ADR fluorescence as measured by ACV indicates a 60% increase in intensity for cells in the early S phase compared to those in G_1 and only a 30% increase for cells in G_2 + M compared to those in S (Fig. 1), suggesting that cells in the early S phase appear to give a higher ADR fluorescence/unit DNA content than those in G_1 or G_2 + M. Published data also indicate that cells in S appear to be most sensitive in terms of cell inactivation [18–20]. Kimler and Cheng observed that the CHO cells in early S and M are very sensitive to ADR whereas the cells in G_1 and G_2 are less sensitive [21].

Due to the cell age-dependence of ADR fluorescence the ADR incorporation in the cell population is not only affected by the influx and efflux of the drug but also by the distribution of the cells through the cell cycle. In addition, during ADR exposure the cell cycle distribution may be affected depending on the dose and exposure period. After briefly exposing synchronized CHO cells to low doses of ADR, Barranco *et al.* found that cells in all phases of the cell cycle except mitosis were delayed [20]. Tobey *et al.* observed that CHO cells treated during G_1 phase progressed through S phase after treatment with high doses of ADR [22]. Göhde *et al.* observed a reduced traversal of CHO cells from G_1 after high doses of ADR treatment [23]. These cytokinetic changes during ADR exposure must be taken into consideration. After brief treatment with low-dose ADR, ADR-resistant V79 cells appear to show minimal changes in the cell-cycle distribution whereas ADR-sensitive cells exhibit a progressive cell cycle perturbation [11]. Thus after low-dose ADR treatment the unperturbed cell cycle distribution will not affect the ADR fluorescence intensity of ADR-resistant cells whereas reduction in the G_1 population of ADR-sensitive cells will be likely to shift the fluorescence profile toward higher ACVs. The degree of shift depends also on the dose and on the duration of exposure. It suggests that a cell population perturbed by other agents would also be likely to show an altered ADR fluorescence as compared to that of an unperturbed population.

In summary, the ADR fluorescence profile and intensity for cells in G_1 are peaked and low, whereas those for cells in early S through M phases are broad and high. The magnitude of intracellular ADR fluorescence appears to be dictated not only by a number of known factors such as drug concentration, exposure period, membrane permeability [1–8] and active drug efflux [9], but also by cell cycle distribution, kinetics of the population during exposure and previous treatment.

Acknowledgements—The authors thank H. Crissman and A. Stevenson for their comments and advice.

REFERENCES

1. Kessel D, Botterill V, Wodinsku I. Uptake and retention of daunomycin by mouse leukemic cells as factors in drug response. *Cancer Res* 1968, **28**, 938–941.
2. Inaba M, Johnson RK. Uptake and retention of adriamycin and daunorubicin by sensitive and anthracycline-resistant sublines of P388 leukemia. *Biochem Pharmacol* 1978, **27**, 2123–2130.

3. Riehm H, Bielder J L. Cellular resistance to daunomycin in Chinese hamster cells. *Cancer Res* 1971, **31**, 409-412.
4. Dano K. Cross resistance between vinca alkaloids and anthracyclines in Ehrlich ascites tumor *in vivo*. *Cancer Chemother Rep* 1972, **56**, 701-708.
5. Biedler JL, Riehm H, Peterson RHF, Spengler BA. Membrane-mediated drug resistance and phenotypic reversion to normal growth behavior of Chinese hamster cells. *JNCI* 1975, **55**, 671-680.
6. Peterson C, Trouet A. Transport and storage of daunorubicin and doxorubicin in cultured fibroblasts. *Cancer Res* 1978, **38**, 4645-4649.
7. Peterson RH, Myers MB, Spengler NA, Biedler JL. Alteration of plasma membrane glycopeptides and gangliosides of Chinese hamster cells accompanying development of resistance to daunorubicin and vincristine. *Cancer Res* 1983, **43**, 222-228.
8. Harris JR, Timberlake N, Henson P, Schimke P, Belli JA. Adriamycin uptake in V79 and adriamycin resistant Chinese hamster cells. *Int J Radiat Oncol Biol Phys* 1979, 5, 1235-1239.
9. Inaba M, Kobayashi H, Sakurai Y, Johnson RK. Active efflux of daunorubicin and adriamycin in sensitive and resistant sublines of P388 leukemia. *Cancer Res* 1979, **39**, 2200-2203.
10. Di Marco A, Arcamone F, Zunino F. Daunorubicin and adriamycin and structural analogues: Biological activity and mechanisms of action. In: Cockran JW, Hahn FH, eds. *Mechanism of Action of Antimicrobial and Antitumor Agents*. Berlin, Springer Verlag, 1975, 101-128.
11. Tokita N, Jett JH, Raju MR, Belli JA. Correlations between cell-cycle perturbations and survival levels after exposure to adriamycin for two Chinese hamster cell lines. *Eur J Cancer Clin Oncol* 1983, **19**, 546-551.
12. Krishan A, Ganapathi R. Laser flow cytometry and cancer chemotherapy: detection of intracellular anthracycline by flow cytometry. *J Histochem Cytochem* 1979, **27**, 1655-1656.
13. Tobey RA. Production and characterization of mammalian cells reversibly arrested in G1 by growth in isoleucine-deficient medium. *Methods Cell Biol* 1973, **VI**, 67-112.
14. Terashima R, Tolmach LJ. X-ray sensitivity and DNA synthesis in synchronous population of Hela cells. *Science* 1963, **140**, 490-492.
15. Holm DM, Cram LS. An improved flow microfluorometer for rapid measurements of cell fluorescence. *Exp Cell Res* 1973, **80**, 105-110.
16 Crissman HA, Tobey RA. Cell-cycle analysis in twenty minutes. *Science* 1974, **184**, 1297-1298.
17. Enger MD, Tobey RA. Effects of isoleucine deficiency on nucleic acid and protein metabolism in cultured CHO cells. Continued ribonucleic acid and protein synthesis in the absence of deoxyribonucleic acid synthesis. *Biochemistry* 1972, **11**, 269-277.
18. Kim SH, Kim JH. Lethal effect of adriamycin on the division cycle of HeLa cells. *Cancer Res* 1972, **32**, 323-325.
19. Drewinko B, Gottlieb JA. Survival kinetics of cultured human lymphoma cells exposed to adriamycin. *Cancer Res* 1973, **33**, 1141-1145.
20. Barranco SC, Gerner EW, Burk KH, Humphrey RM. Survival and kinetics effects of adriamycin on mammalian cells. *Cancer Res* 1973, **33**, 11-16.
21. Kimler BF, Cheng CC. Comparison of the effects of dihydroxyanthraquinone and adriamycin on the survival of cultured Chinese hamster cells. *Cancer Res* 1982, **42**, 3631-3636.
22. Tobey RA, Crissman HA, Oka MS. Arrested and cycling CHO cells as a kinetic model: studies with adriamycin. *Cancer Treat Rep* 1976, **60**, 1829-1837.
23. Göhde W, Meistrich M, Meyne R, Schumann J, Johnston D, Barlogie B. Cell-cycle induced cell progression delay. *J Histochem Cytochem* 1979, **27**, 470-473.